PHILOSOPHICAL TRANSACTIONS A

Phil. Trans. R. Soc. A.
doi:10.1098/not yet assigned

Sampling effects in QM/MM Trajectory Surface Hopping Nonadiabatic Dynamics

Davide Avagliano*[1,†], Emilio Lorini[1], Leticia González*[1,2]

[1]*Institute of Theoretical Chemistry, Faculty of Chemistry, University of Vienna, Währinger Straße 17, A-1180 Vienna, Austria*
[2]*Vienna Research Platform on Accelerating Photoreaction Discovery, University of Vienna, Währinger Straße 17, A-1180 Vienna, Austria*

Keywords: Surface hopping, QM/MM, initial conditions

Summary

The impact of different initial conditions in nonadiabatic trajectory surface hopping dynamics within a hybrid quantum mechanical/molecular mechanics scheme is investigated. The influence of a quantum sampling, based on a Wigner distribution, a fully thermal sampling, based on classical molecular dynamics, and a quantum sampled system, but thermally equilibrated with the environment, are investigated on the relaxation dynamics of solvated fulvene after light irradiation. We find that the decay from the first singlet excited state to the ground state shows high dependency on the initial condition and simulation parameters. The three sampling methods lead to different distributions of initial geometries and momenta, which then affect the fate of the excited state dynamics. We evaluated both the effect of sampling geometries and momenta, analysing how the ultrafast decay of fulvene changes accordingly. The results are expected to be of interest to decide how to initialise nonadiabatic dynamics in the presence of the environment.

*Authors for correspondence (davide.avagliano@unibo.it and leticia.gonzalez@univie.ac.at).

†Present address: Dipartimento di Chimica Industriale "Toso Montanari", Università degli Studi di Bologna, Viale Del Risorgimento, 4, I-40136 Bologna, Italy

Introduction

Trajectory Surface Hopping (TSH) is a widely used method to simulate excited states nonadiabatic dynamics (1,2). The method is based on the propagation of an ensemble of independent trajectories, which evolve individually with the nuclei propagated following Netwon's law of motion on potential energy surfaces (PES) calculated on-the-fly. When a trajectory is in the proximity of a conical intersection (3), the nonadiabatic effects arising from the coupling among nuclear and electronic motions are approximated so that either a switch takes place between two electronic states through instantaneous hops or the trajectory keeps propagating on the same surface. Through a statistically reasonable ensemble of trajectories it is possible to mimic the behaviour of a splitting wave packet (4). Despite its approximations, surface hopping has become very popular as it allows the description of the excited states dynamics of many systems, from small to large, depending on the underlying expense involved in the method employed to calculate the PES on-the-fly. Here one can choose from the large variety of quantum mechanical methods (QM) (5) or resort to semiempirical approximations(6). Yet, when solvent and environmental effects need to be considered, further approximations are required (7). One smart way to consider the interaction between a molecule and its environment is to treat them at different levels of theory. In its simplest form, the chromophore can be treated with QM at high level of theory, while the energy of other parts of the system and the solvent molecules can be calculated by means of classical force fields. This approach is known as quantum mechanical/molecular mechanics (QM/MM) (8) and it is efficiently used to include environmental effects in ground and electronically excited states simulations (9).

One important ingredient in TSH simulations is the generation of initial conditions, i.e. the sampling of the distribution of positions and momenta. Interestingly, it has been shown that this can influence the results of the nuclear dynamics obtained (10,11). One approach to generate initial conditions is to sample thermally the configurational space, where the vibrational energy for each normal mode is given by k_bT, obtained with a classical or ab-initio molecular dynamics in the electronic ground state. This approach neglects quantum effects, like the zero-point energy (ZPE), which is instead included if a quantum sampling of the phase space is employed. Here, a common approach is to calculate a Wigner distribution of probability densities of positions and momenta for each normal mode (12). Additionally, several approaches combining (13) or improving (14) the aforementioned approaches to obtain position and velocities distributions have been lately developed. While these different ways of sampling have been tested and compared in the past for surface-hopping dynamics in the gas phase (10), the situation becomes more complex within a QM/MM scheme, where the chromophore interacts with the environment, and it is in thermal equilibrium with it (15). In this work we want to investigate the effect of different methodologies for sampling the initial conditions in TSH trajectories but applied to a QM/MM framework. As a test case, we choose fulvene, which undergoes ultrafast dynamics and has been well studied in the past in the gas phase (16–19). After population of the first electronically excited state, fulvene can relax to the electronic ground state through two conical intersections, a peaked and a sloped one, which are associated to the torsion and the stretching of the C=C alkene bond, respectively. The sloped conical intersection allows for a reflection of the population, which comes back to the S_1. For this reason, fulvene has been recently proposed as a molecular model (20) to describe nonadiabatic processes, in particular reflection of population on excited states PES, in analogy to the two dimensional model proposed by Tully in 1990 (1).

Interestingly, the authors of Ref. (20) showed that the decay and reflection through the sloped conical intersection or the relaxation through the peaked one is strongly dependent on the simulation parameters. This motivated us to investigate whether modulating the initial conditions can also change the dynamics of fulvene in water. The non-polarity of the molecule helps us to focus on the dynamical behaviour induced exclusively by the change of the different initial values of the vibrational kinetic energy (KE) and geometries, by avoiding physical (for instance hydrogen bonds) interactions between the chromophore and the solvent throughout the course of the dynamics. We limit the solvent role to electrostatic effects, yet analogous for each set of generated initial conditions. For these calculations we shall use our recently developed scheme to run QM/MM nonadiabatic dynamics simulations (21) based on SHARC (22,23) and COBRAMM (24,25) software, which provide TSH and the QM/MM implementations, respectively. We will show how changing the initial momenta, either due to manual selection or through energy exchange and equilibration between the QM and the MM region, will lead to very different and interesting results that should be kept in mind when deciding how to sample initial conditions for QM/MM TSH simulations.

Methods

Sampling methods

We shall consider six different sets of ensembles of initial conditions, schematically depicted in Figure 1. First, we calculated a Wigner distribution of the QM part to sample the ground state phase space of isolated fulvene. The solvent effects on the distribution are considered by optimising the geometry and calculating the normal modes including the effect of water by implicit solvation (26) with a polarizable continuum scheme (PCM).

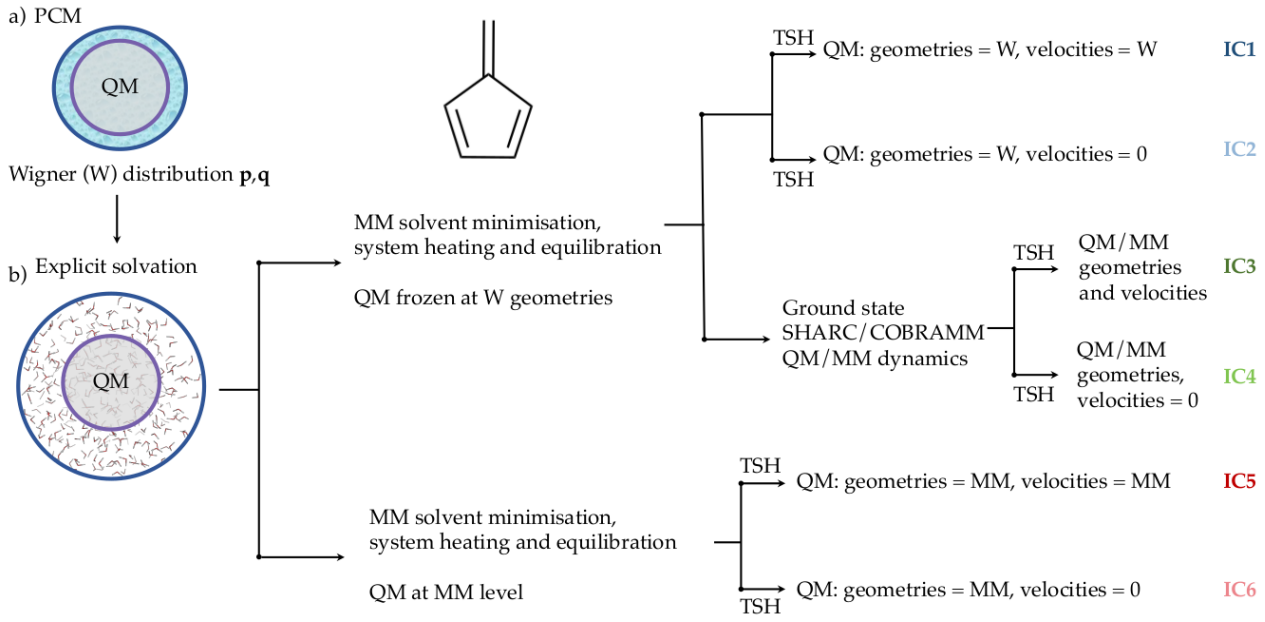

Figure 1: Schematic representation of the generation of six different ensembles of initial conditions (IC1-6) for QM/MM nonadiabatic dynamics.

We then solvated each of the geometries obtained with explicit water molecules. We optimised, heated and equilibrated each individual geometry. In a first case, we did these steps keeping the QM part frozen at the Wigner geometries. The first TSH set of trajectories is then initialised from Wigner geometries and velocities, surrounded by MM water molecules (IC1). In Ref. (20) it was shown that, in the gas phase, sloped CI can be reached more efficiently over the peaked one if the velocities are set to zero. In order to test this effect in water, we initialised a second set of trajectories from Wigner geometries with the velocities set to zero (IC2). Additionally, we took the solvated QM geometries and from the Wigner positions and momenta we ran a ground-state post-equilibration at the QM/MM level with the SHARC/COBRAMM scheme during 100 fs. After that, we initialised a third set of trajectories (IC3). As in the previous case, an additional set, where the velocities were set to zero, was also prepared (IC4). Last family of initial conditions was fully thermally sampled. Starting from the solvated molecules, we minimised, heated and equilibrated the system at MM level, including the QM part treated at the force field level. At the end of the equilibration two sets of trajectories were initialized, one with geometries and velocities obtained at the MM level for the whole system (IC5) and one with geometries at MM level and again velocities set to zero (IC6). Summarizing, we sampled the QM region at a quantum level (IC1 and IC2), with a quantum system, but with the vibration relaxed and equilibrated with the surrounding water molecules (IC3 and IC4) and with a full thermal sampling obtained by classical molecular mechanics (IC5 and IC6).

QM/MM scheme

The QM/MM scheme used in this work follows the recent (19) implementation resulting from interfacing SHARC and COBRAMM. Highlights in the QM/MM implementation include; i) a subtractive scheme for the calculation of the energy and the gradient of the electronic states(8), with the implementation of an electrostatic embedding scheme (27) to account for the polarisation of the QM part due to the presence of the surrounding MM environment, included in the adopted Hamiltonian as point charges; ii) the inclusion in the MM gradient of a state-specific term due to the force induced by the QM region on the point charges; iii) the QM molecule surrounded by a droplet of homogeneous radius of water molecules and, in order to address the lack of periodical boundary conditions, the external shell of water molecules is kept frozen to furnish a constant potential and keep the droplet stable. Additional information and the full implementation can be found in the original publication (21).

Computational details

All the QM calculations were performed with the complete active space self-consistent field (CASSCF) (28) using six electrons in six active orbitals, combined with a 6-31G* basis set (29), denoted as CASSCF(6,6)/6-31G* level of theory. The active orbitals are the 3 π and 3 π^* orbitals of the fulvene. These calculations are performed with the OpenMolcas software (30). The quantum distribution of the electronic ground state of the QM geometries and velocities was obtained at the fulvene optimised geometry where each of the normal modes was sampled with a harmonic quantum Wigner oscillator. The sampling was performed at 300 K to include the possible population of different vibrational states (31) and the effect of the environment was included in the optimisation of the molecule and the computation of the normal modes with PCM, (26) as implemented in OpenMolcas. A

total amount of 500 geometries obtained was solvated with a box of water molecules and the system was minimised for 500 cycles with the steepest descent algorithm and for 2000 with the conjugated gradient method. After that the systems were heated at 300K in 50 ps, pressure and volume were equilibrated for 100 ps with the temperature kept constant to 300K with a Nosé-Hoover thermostat (32). During these steps, the QM part was kept frozen at the initial geometry obtained from the Wigner distribution and, at the end of this setup, a droplet of 500 solvent molecules was stripped around the centred chromophore. All the MM calculation were carried out with AMBER suite (33).

At this stage, we obtained the six different ensembles of initial conditions for TSH. For each of it, the same TSH parameters (see below) were adopted. We ran 500 independent trajectories from all the 500 Wigner geometries that we solvated. The simulation time was 70 fs, with a nuclear time step of 0.5 fs. Only two states, S_1 and S_0, were included. The nonadiabatic coupling was approximated by evaluating the time-derivative coupling through wavefunction overlaps (34). The energy based decoherence correction scheme (35), with a decoherence parameter of 0.1, and an atom masking to exclude the solvent molecules from the velocities rescaling procedures was employed (21).

The water molecules were treated with the flexible force field SPC/Fw (36), as available in AMBER. During the SHARC/COBRAMM dynamics, the 300 molecules of the droplet closest to the QM part were allowed to move, while the most external 200 ones were kept frozen. For IC5 and IC6, the setup steps were analogous, with the difference that the chromophore was allowed to move under the effect of the classical general AMBER force fields (GAFF) potentials (37) and the TSH was initialised from the last snapshot of the equilibration procedure.

Results and discussion

Theoretical studies in gas phase (17–19) showed that, after the population of the first electronic excited state, fulvene undergoes a double-decay relaxation within the first tens of fs. Interestingly, the preference for one or the other competitive decay pathway can be strongly influenced by the initial conditions and the simulation parameters chosen to initialise and propagate the excited states dynamics (20). In reference (20), the authors showed how the reflective conical intersection, connected to the stretching of the $C{=}CH_2$ bond, is easily reached in TSH simulations when the velocities of the initial geometries were set to zero. In our reference gas phase TSH dynamics (Figure 2a), we observed the decay to S_0 within the first 10 fs and the population reflected to S_1 within in the first 30 fs in both dynamics --initialising the trajectories from Wigner velocities or velocities set to zero-- but with a notably increased reflection in the second case. Note that our simulations employ a different number of trajectories than Ref. (20) and that we use 250 different initial geometries. Additionally, we extended the dynamics up to 70 fs, including two more reflection cycles.

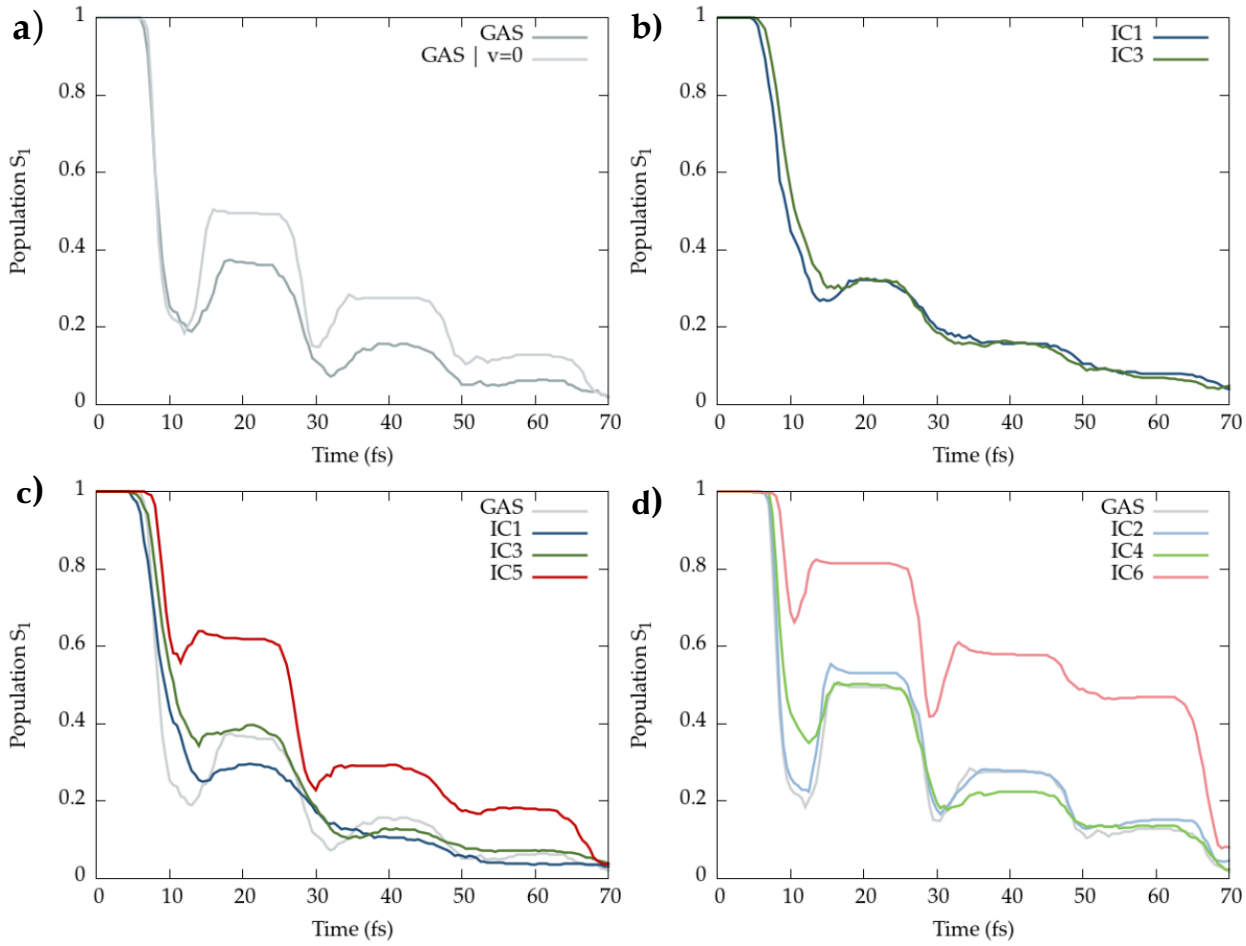

Figure 2: Time-resolved population of the first excited state (S_1) for the different ensemble of trajectories: a) population of 250 gas phase trajectories starting from initial velocities obtained from a Wigner distribution (GAS) or set to zero (GAS | v=0); b) population relative to 500 QM/MM trajectories, with all the 500 water molecules kept frozen, for IC1 and IC3; c) population relative to 500 QM/MM trajectories with 300 water molecules allowed to move and the most external 200 ones frozen for IC1, IC3 and IC5 and d) analogous population obtained from IC2, IC4 and IC6.

Having obtained a general picture in gas phase, we can now move to study the effect of the QM/MM setups on the dynamics. We first proceed to evaluate the pure electronic effect of the presence of the solvent. For this purpose, we first ran TSH dynamics with IC1 and IC3, but keeping frozen all the solvent molecules and letting the fulvene move in a constant static potential given by the same point charges distribution (Figure 2b). Note that, in this example, in the case of IC3, both in the ground state equilibration and in the TSH the water molecules are kept frozen. Regardless of whether we initialise the dynamics directly from the Wigner position and momenta (IC1) or we take the same initial conditions and first ran a ground-state dynamics (IC3), the S_1 population profiles decay very similarly. In both cases, the decay time to S_0 does not change with respect to the gas phase, but the inversion of population within the first 30 fs is reduced and fully disappears in the next two reflection cycles. A slight difference between the dynamics based on IC1 and IC3 is present in the population around 15 fs. While IC1 shows a bit of inversion of the population trend, IC3 shows a fully flat population. However, both decays continue flatly and constant without showing any reflection from 25 to 70 fs in the

presence of the electrostatic potential induced by the water. We had nevertheless expected that including the interaction of the QM part with a shell of mobile explicit water molecules, would affect the TSH dynamics. Indeed, the equilibration of the vibrational modes of the QM molecule includes the interaction with the solvent molecule, and the thermal equilibration of the whole system accounts for the equilibration of the water degrees of freedom. In this sense, the choice of a flexible force field is fundamental, allowing the stretching of the O-H bonds of the solvent molecules, which would otherwise be constrained in the case of a rigid model, such as the common TIP3P choice (38). Such constraint would remove vibrational modes of the solvent molecules from the thermal equilibration, altering the changes in vibrational energy distribution of the QM part, and we would not include the interactions of all the solvent normal modes on the position and momenta distributions of fulvene.
In addition to the general effect of the explicit mobile waters, we expected differences in the dynamics according to the different sets of distributions of IC. Indeed, the ensemble of geometries obtained with the three sampling methods (quantum, quantum plus thermal equilibration, fully thermal) came out to be rather different from each other (Figure 3a) and so is the kinetic energy of the associated QM part (Figure 3b). The Wigner distribution is obtained for the normal modes at the optimized geometry, but once the molecule is allowed to relax from this frozen geometry in the presence of the water, it displaces its normal modes over the conformational space (Figure 3a). At the same time, it gets colder due to the thermal equilibration with the surrounding solvent molecules, as can be seen by the decrease of the averaged initial KE of the QM part for IC3 that is halved with respect of IC1 (Figure 3b). In contrast, the full classical thermal sampling produces a sampling more limited in the conformational space (Figure 3a). This sampling method of IC5 produces a much colder QM part. Indeed, in IC5, fulvene increase its KE during the TSH dynamics while interacting with the solvent molecules (Figure 3b).
The differences in initial KE among IC1, IC3 and IC5 are reflected in their S_1 population decays (Figure 2). Compared to IC1 driven dynamics, that from IC3 leads to 10% more population trapped in the S_1 state between 10 and 30 fs (Figure 2c). This difference in population, which was absent in the case of frozen water molecules, it can be ascribed to the equilibration with the solvent along the ground state QM/MM dynamics. Nonetheless, in both IC1 and IC3 cases, the population profile is flat and does not show the same reflection found in the gas phase. After 30 fs, in both cases the S_1 population decays to the ground state similarly along the torsional path, without showing any reflection. The situation drastically changes for IC5, where the chromophore was treated classically (Figure 2c). Here, after 10 fs, only 40% of the population is transferred to S_0, in contrast to the almost 80% and 60% of IC1 and IC3, respectively. The reflection to S1 is now more pronounced, making the S_1 population between 10 and 30 fs approximately double than in case of IC1. Two reflection cycles are clearly present during the rest of the dynamics. The lower KE, the absence of ZPE and the harmonic classical potential used for this sampling, they all make the relaxation less pronounced and passing through the sloped CI. In order to exclude the possibility that such differences in population are not an artifact of the decoherence correction scheme used, where the damping of the electronic coefficient is based on the KE value of the chromophore, we have re-ran the same trajectories for IC1 with different decoherence parameters (instead of default 0.1, set to 0.3 and 0.7 in this test). We found (results not shown) that the population profile remains the same and do not

converge to the one of IC3 or IC5 thus excluding unphysical artifacts due to the decoherence correction scheme employed.

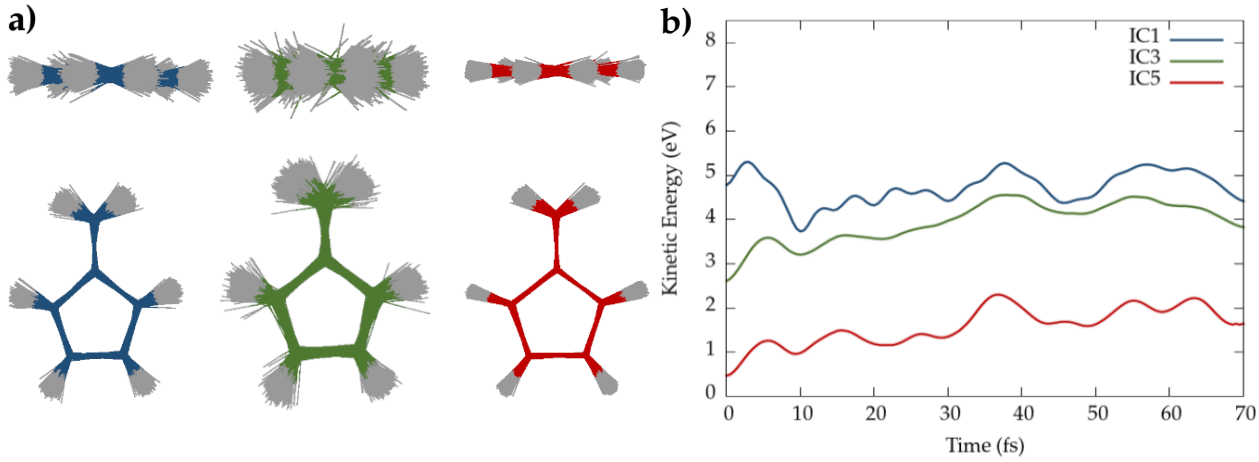

Figure 3: a) Cluster of 500 initial geometries obtained by different sampling methods: left and blue IC1, middle and green IC3 and right and red IC5; b) averaged kinetic energy of the QM region during the TSH dynamics for IC1, IC3 and IC5.

Regarding fulvene dynamics in the gas phase, it was shown that setting the initial velocities to zero made easier to reach the sloped CI, leading to a strong reflection of the population in the first tens of fs. Now, we want to investigate whether this effect is also present within the QM/MM setups (Figure 2d). Setting the momenta always to zero, the differences among IC2, IC4 and IC6 should mainly reflect the differences in the sampling on the conformational space, helping to disentangle and discriminate the effect of the sampled geometries or velocities. As anticipated, in all IC2, IC4 and IC6-based dynamics, the sloped CI is now easily reached (Figure 2d) and the system shows high degree of reflection to S_1 once S_0 is populated. IC2 leads basically to the same dynamics as in gas phase, with the same behaviour along the whole dynamics and the same degree of reflection. However, IC4 triggers a strong reflection in the 10-30 fs region, while the S_1 population is flat when using IC3. In all IC2, IC4 and IC6, the decay along the sloped CI is followed also during the rest of the dynamics, with the respective proportion among the three reflection cycles. IC6 induces an enhancement of the S_1 population in the region of the first reflection and, as was the case for IC5, only a small fraction of the population decays to the ground state within first 10 fs. A clear second reflection is present between 30 and 50 fs and half of the population is still in the first excited states along the first 60 fs. The full classical sampling of the QM geometries produces a slower relaxation from the S_1 and a prevalence of the relaxation through the sloped CI over the peaked one, as can be seen be similar features present in both IC5 and IC6 driven S_1 population profiles. In both, fully quantum sampling and quantum followed by thermal relaxation, the presence of the environment leads the dynamics through the peaked CI, with no substantial differences when the water molecules are frozen. This is confirmed by clustering the hopping geometries for the first S_1 -> S_0 transition (Figure 4) and comparing with the averaged values of the C=CH_2 and C-C=C-H torsion (Table 1).

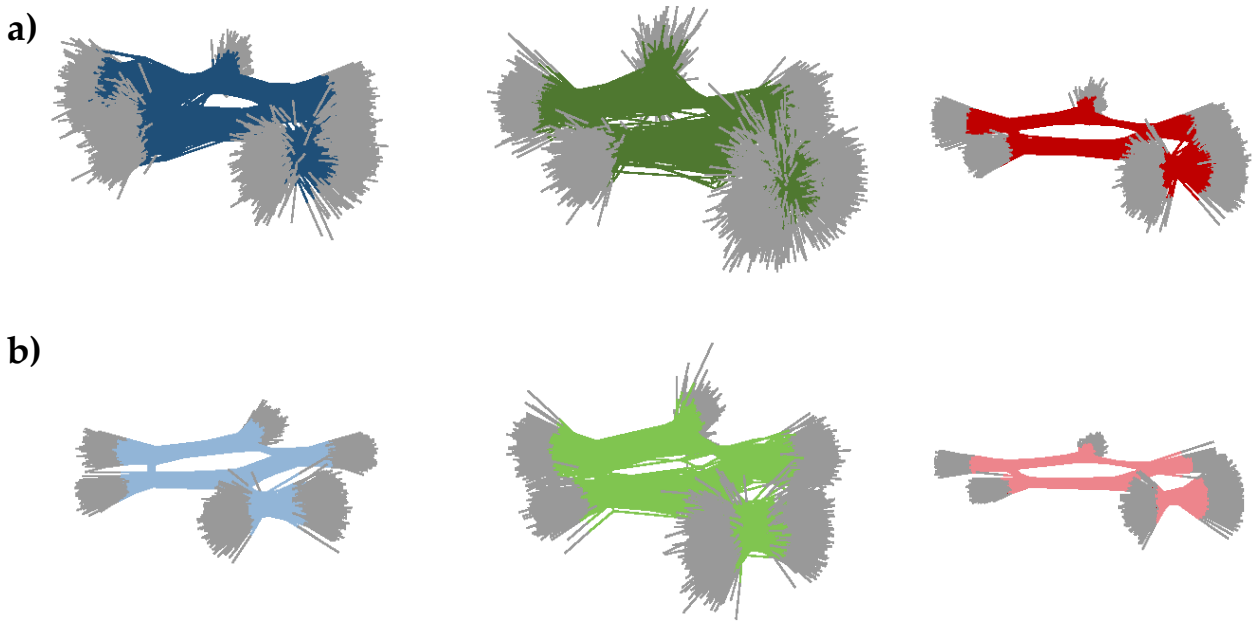

Figure 4: Cluster of hopping geometries from S_1 to S_0 around 10 fs for a set of trajectories starting from a) IC1 (dark blue, left), IC3 (dark green, middle) and IC5 (dark red, right) and starting from b) set of trajectories with null initial momenta IC2 (light blue, left), IC4 (light green, middle) and IC6 (light red, red).

The hopping geometries result to be very different between IC1, IC3 and IC5, with only the last one keeping the original planarity. The value of the averaged torsional for the S1 -S0 hopping shows how, the more the molecule is bent, the more likely the path through the peaked CI is (Table 1). Indeed, the C=CH_2 stretching value does not change for any of the cluster of the hopping geometries, while the difference in initial momenta, consequence of the different samplings, influences the motion of the torsion and the energy of that mode. Interestingly, the equilibration with the solvent in the ground state of the Wigner geometries, on the one hand side makes the chromophore colder, and thus shows a decrease of KE (Figure 3b), but on the other side redistributes the vibrational energy and allows stronger torsion. Setting the initial velocities to zero, keeps the orientation of the hopping geometries within the first 10 fs as the initial one, resulting in IC2 and IC6 still very planar, but IC4 distorted by the previous interaction with the solvent molecules during the grounds state dynamics (Figure 4b).

	C=CH_2 (Å)		C-C=C-H (°)	
	initial	S_1->S_0 hop	initial	S_1->S_0 hop
IC1	1.36	1.56	9.05	22.52
IC2		1.59		11.01
IC3		1.59		24.82

IC4	1.35	1.59	13.06	14.77
IC5	1.35	1.58	5.25	15.95
IC6		1.59		9.72

Table 1: Averaged values of the C=CH_2 stretching and the C-C=C-H torsion for all the initial conditions sets at time step t=0 (initial) and the hopping geometry of the first S_1 -> S_0 relaxation within 10 fs

In summary, we have shown that changing the sampling method can strongly influence the geometrical distribution, the energetics and thus the evolution of the trajectories. Despite such an awareness is present in gas phase excited state dynamics(10), attention is needed when explicit solvent and environmental interactions are considered. This is particularly true when two different levels of theory are combined, such as in the multiscale QM/MM schemes. Often, the high number of degrees of freedom to be described and the high flexibility of the chromophore force a thermal sampling, typically based on classical molecular dynamics simulations. A full thermal sampling is ran using approximated harmonic potentials, it misses the ZPE and produces a colder system, that prevents high energy modes to be properly sampled. The latter problem can also be tackled by a local reheating (39), but such an approach still lacks quantum effects in the phase space distributions. A full quantum sampling, obtained for example with a Wigner probability distribution, is a double-edged knife, as it considers quantum effects like the ZPE, but often delivers too high energy modes, a distribution limited to a single minimum geometry, and the impossibility of explicitly account for the interaction with solvent molecules. An interesting alternative approach is the one we adopted in the IC3 setup. By employing a QM/MM ground-state molecular dynamics, the Wigner geometries and momenta of the chromophore are equilibrated with the solvent degrees of freedom; in this way, IC3 allows to keep the information relative to the ZPE, to redistribute vibrational energy along the lower energy vibrational modes, and to account for a direct interaction and polarisation of the explicit solvent molecules. Therefore, we believe that the approach employed in IC3 is a reasonable compromise out of the different sampling methods and the most suitable for QM/MM TSH setups. At the same time, we are aware these sampling methods are not the only possibly way to generate initial condition for semi-classical nonadiabatic dynamics. Mixed classical-quantum methods have been highly promising to describe the shape of the UV absorption of dyes (40,41) or more complicated systems as transition metal complexes (39) or biological structures (42) in explicit solvent environments. It would be interesting to compare their applicability along nonadiabatic dynamics simulations. Further, sampling methods that include laser fields in order to better reproduce wavepackets formed by laser experiments have been also developed (43) and it would be interesting to see their extension to a QM/MM framework.

Conclusions

In this work we applied our recently developed approached for running QM/MM TSH simulations, based on the interface of SHARC and COBRAMM codes, to study an apparently simple, yet delicate aspect of nonadiabatic dynamics: the generation of initial conditions. If the complexity of this task is non-trivial in gas phase calculations, we show here that even more care is needed when solvent degrees of freedom and their interaction with the chromophore are also included in the sampling of the QM part within hybrid QM/MM approaches. We compared the dynamical effects of employing: i) a quantum approach, based on Wigner sampling and successive solvent relaxation, ii) a quantum approach but thermally relaxed, with the Wigner position and momenta equilibrated with the surrounding mobile environment, and iii) a fully thermal sampling, completely relying on classical force field potentials. The three sampling approaches show important differences given by the initial values chosen to initialize the dynamics, as evident in the S_1 relaxation decay of a proof-of-concept molecule, fulvene. The first S_1 -> S_0 decay occurs for all the cases within the first 10fs, but the amount of population transferred to the ground state changes according to different sets of geometries and initial KE (IC5 > IC3 > IC1). The higher initial momenta the QM part has, the more prompt is to decay to S_0 through a peaked CI, while a lower amount of KE induces more the decay through the sloped CI connected to the $C{=}CH_2$, with annexed reflection and population transfer back to the S_1. As in gas phase, this reflection is enhanced by setting the initial momenta to zero, but with clear differences in the amount of population transferred according to the initial geometry sampled (IC6 > IC4 > IC2). The different sampling methods showed differences in the initial KE, in the portion of conformational space sampled, and consequently, in the evolution of the excited state dynamics.

We thus demonstrate that is essential to ponder the choice of the initial conditions, with their pros and cons, and their possible effects on the nuclear dynamics. The explicit effect of the environment increases the difficulties to make a meaningful choice. With this work, we presented an comprehensive comparison among possible sampling methods compatible with a QM/MM approach and disentangled the role of the geometries and velocities differently sampled. We hope that this work will stimulate further analyses and will contribute to the success of running meaningful TSH QM/MM dynamics with suitable set of initial conditions.

Additional Information

Authors' Contributions
DA and LG conceived of and designed the study, EL carried out all the calculations. DA and EL carried out the analysis. DA drafted the manuscript. LG revised the draft. All authors read and approved the manuscript.

Data Accessibility
All data is original, not published before. The codes used SHARC and COBRAMM are open-access. Initial conditions files, exemplary input and S1 populations for IC1 with different decoherence parameter are available under free license at https://phaidra.univie.ac.at/search#?page=1&pagesize=10&owner=avaglianod92

Competing Interests
The authors declare that they have no competing interests.

Funding Statement
DA and LG thank funding from the European Union's Horizon 2020 research and innovation program under the Marie Sklodowska-Curie grant agreement no. 765266 (LightDyNAmics). EL thank the Erasmus program for supporting his visit to the University of Vienna.

Acknowledgments
The University of Vienna and the Vienna Scientific Cluster (VSC) are acknowledged for allocation of computational resources.

References

1. Tully JC. Molecular dynamics with electronic transitions. J Chem Phys [Internet]. 1990 Jul 15;93(2):1061–71. Available from: https://doi.org/10.1063/1.459170
2. Tully JC, Preston RK. Trajectory Surface Hopping Approach to Nonadiabatic Molecular Collisions: The Reaction of H+ with D2. J Chem Phys [Internet]. 1971 Jul 15;55(2):562–72. Available from: https://doi.org/10.1063/1.1675788
3. Bernardi F, Olivucci M, Robb MA. Potential energy surface crossings in organic photochemistry. Chem Soc Rev [Internet]. 1996;25(5):321–8. Available from: http://dx.doi.org/10.1039/CS9962500321
4. Barbatti M. Nonadiabatic dynamics with trajectory surface hopping method. WIREs Comput Mol Sci [Internet]. 2011 Jul 1;1(4):620–33. Available from: https://doi.org/10.1002/wcms.64
5. Mai S, González L. Molecular Photochemistry: Recent Developments in Theory. Angew Chemie Int Ed [Internet]. 2020 Sep 21;59(39):16832–46. Available from: https://doi.org/10.1002/anie.201916381
6. Thiel W. Semiempirical quantum–chemical methods. WIREs Comput Mol Sci [Internet]. 2014 Mar 1;4(2):145–57. Available from: https://doi.org/10.1002/wcms.1161
7. Santoro F, Green JA, Martinez-Fernandez L, Cerezo J, Improta R. Quantum and semiclassical dynamical studies of nonadiabatic processes in solution: achievements and perspectives. Phys Chem Chem Phys [Internet]. 2021;23(14):8181–99. Available from: http://dx.doi.org/10.1039/D0CP05907B
8. Senn HM, Thiel W. QM/MM Methods for Biomolecular Systems. Angew Chemie Int Ed [Internet]. 2009 Feb 2;48(7):1198–229. Available from: https://doi.org/10.1002/anie.200802019
9. Morzan UN, Alonso de Armiño DJ, Foglia NO, Ramírez F, González Lebrero MC, Scherlis DA, et al. Spectroscopy in Complex Environments from QM–MM Simulations. Chem Rev [Internet]. 2018 Apr 11;118(7):4071–113. Available from: https://doi.org/10.1021/acs.chemrev.8b00026
10. Barbatti M, Sen K. Effects of different initial condition samplings on photodynamics and spectrum of pyrrole. Int J Quantum Chem [Internet]. 2016 May 15;116(10):762–71. Available from: https://doi.org/10.1002/qua.25049
11. Zobel JP, Heindl M, Nogueira JJ, González L. Vibrational Sampling and Solvent Effects on the Electronic Structure of the Absorption Spectrum of 2-Nitronaphthalene. J Chem Theory Comput [Internet]. 2018 Jun 12;14(6):3205–17. Available from: https://doi.org/10.1021/acs.jctc.8b00198

12. Dahl JP, Springborg M. The Morse oscillator in position space, momentum space, and phase space. J Chem Phys [Internet]. 1988 Apr 1;88(7):4535–47. Available from: https://doi.org/10.1063/1.453761
13. Sun L, Hase WL. Comparisons of classical and Wigner sampling of transition state energy levels for quasiclassical trajectory chemical dynamics simulations. J Chem Phys [Internet]. 2010 Jul 28;133(4):44313. Available from: https://doi.org/10.1063/1.3463717
14. Yao Y, Hase WL, Granucci G, Persico M. Sampling initial positions and momenta for nuclear trajectories from quantum mechanical distributions. J Chem Phys [Internet]. 2021 Feb 19;154(7):74115. Available from: https://doi.org/10.1063/5.0039592
15. Klaffki N, Weingart O, Garavelli M, Spohr E. Sampling excited state dynamics: influence of HOOP mode excitations in a retinal model. Phys Chem Chem Phys [Internet]. 2012;14(41):14299–305. Available from: http://dx.doi.org/10.1039/C2CP41994G
16. Mendive-Tapia D, Lasorne B, Worth GA, Robb MA, Bearpark MJ. Towards converging non-adiabatic direct dynamics calculations using frozen-width variational Gaussian product basis functions. J Chem Phys [Internet]. 2012 Nov 27;137(22):22A548. Available from: https://doi.org/10.1063/1.4765087
17. Mendive-Tapia D, Lasorne B, Worth GA, Bearpark MJ, Robb MA. Controlling the mechanism of fulvene S1/S0 decay: switching off the stepwise population transfer. Phys Chem Chem Phys [Internet]. 2010;12(48):15725–33. Available from: http://dx.doi.org/10.1039/C0CP01757D
18. Alfalah S, Belz S, Deeb O, Leibscher M, Manz J, Zilberg S. Photoinduced quantum dynamics of ortho- and para-fulvene: Hindered photoisomerization due to mode selective fast radiationless decay via a conical intersection. J Chem Phys [Internet]. 2009 Mar 28;130(12):124318. Available from: https://doi.org/10.1063/1.3089546
19. Bearpark MJ, Bernardi F, Olivucci M, Robb MA, Smith BR. Can Fulvene S1 Decay Be Controlled? A CASSCF Study with MMVB Dynamics. J Am Chem Soc [Internet]. 1996 Jun 5;118(22):5254–60. Available from: https://doi.org/10.1021/ja9542799
20. Ibele LM, Curchod BFE. A molecular perspective on Tully models for nonadiabatic dynamics. Phys Chem Chem Phys [Internet]. 2020;22(27):15183–96. Available from: http://dx.doi.org/10.1039/D0CP01353F
21. Avagliano D, Bonfanti M, Garavelli M, González L. QM/MM Nonadiabatic Dynamics: the SHARC/COBRAMM Approach. J Chem Theory Comput [Internet]. 2021 Jun 11; Available from: https://doi.org/10.1021/acs.jctc.1c00318
22. Mai S, Marquetand P, González L. A general method to describe intersystem crossing dynamics in trajectory surface hopping. Int J Quantum Chem [Internet]. 2015 Sep 15;115(18):1215–31. Available from: https://doi.org/10.1002/qua.24891
23. S. Mai, M. Richter, M. Heindl, M. F. S. J. Menger AJA, M. Ruckenbauer, F. Plasser, L. M. Ibele, S. Kropf, M. Oppel PM, González L. SHARC2.1: Surface Hopping Including Arbitrary Couplings – Program Package for Non-Adiabatic Dynamics. sharc-md.org. 2019.
24. Altoè P, Stenta M, Bottoni A, Garavelli M. A tunable QM/MM approach to chemical reactivity,

structure and physico-chemical properties prediction. Theor Chem Acc [Internet]. 2007;118(1):219–40. Available from: https://doi.org/10.1007/s00214-007-0275-9

25. Weingart O, Nenov A, Altoè P, Rivalta I, Segarra-Martí J, Dokukina I, et al. COBRAMM 2.0 — A software interface for tailoring molecular electronic structure calculations and running nanoscale (QM/MM) simulations. J Mol Model. 2018;
26. Barone V, Cossi M. Quantum Calculation of Molecular Energies and Energy Gradients in Solution by a Conductor Solvent Model. J Phys Chem A [Internet]. 1998 Mar 1;102(11):1995–2001. Available from: https://doi.org/10.1021/jp9716997
27. Dohn AO. Multiscale electrostatic embedding simulations for modeling structure and dynamics of molecules in solution: A tutorial review. Int J Quantum Chem [Internet]. 2020 Nov 1;120(21):e26343. Available from: https://doi.org/10.1002/qua.26343
28. Roos BO, Taylor PR, Sigbahn PEM. A complete active space SCF method (CASSCF) using a density matrix formulated super-CI approach. Chem Phys [Internet]. 1980;48(2):157–73. Available from: https://www.sciencedirect.com/science/article/pii/0301010480800450
29. Ditchfield R, Hehre WJ, Pople JA. Self-Consistent Molecular-Orbital Methods. IX. An Extended Gaussian-Type Basis for Molecular-Orbital Studies of Organic Molecules. J Chem Phys [Internet]. 1971 Jan 15;54(2):724–8. Available from: https://doi.org/10.1063/1.1674902
30. Fdez. Galván I, Vacher M, Alavi A, Angeli C, Aquilante F, Autschbach J, et al. OpenMolcas: From Source Code to Insight. J Chem Theory Comput [Internet]. 2019 Nov 12;15(11):5925–64. Available from: https://doi.org/10.1021/acs.jctc.9b00532
31. Zobel JP, Nogueira JJ, González L. Finite-temperature Wigner phase-space sampling and temperature effects on the excited-state dynamics of 2-nitronaphthalene. Phys Chem Chem Phys [Internet]. 2019;21(26):13906–15. Available from: http://dx.doi.org/10.1039/C8CP03273D
32. Martyna GJ, Klein ML, Tuckerman M. Nosé–Hoover chains: The canonical ensemble via continuous dynamics. J Chem Phys [Internet]. 1992 Aug 15;97(4):2635–43. Available from: https://doi.org/10.1063/1.463940
33. Salomon-Ferrer R, Case DA, Walker RC. An overview of the Amber biomolecular simulation package. WIREs Comput Mol Sci [Internet]. 2013 Mar 1;3(2):198–210. Available from: https://doi.org/10.1002/wcms.1121
34. Plasser F, Ruckenbauer M, Mai S, Oppel M, Marquetand P, González L. Efficient and Flexible Computation of Many-Electron Wave Function Overlaps. J Chem Theory Comput [Internet]. 2016 Mar 8;12(3):1207–19. Available from: https://doi.org/10.1021/acs.jctc.5b01148
35. Granucci G, Persico M. Critical appraisal of the fewest switches algorithm for surface hopping. J Chem Phys [Internet]. 2007 Apr 5;126(13):134114. Available from: https://doi.org/10.1063/1.2715585
36. Wu Y, Tepper HL, Voth GA. Flexible simple point-charge water model with improved liquid-state properties. J Chem Phys [Internet]. 2006 Jan 10;124(2):24503. Available from: https://doi.org/10.1063/1.2136877
37. Wang J, Wolf RM, Caldwell JW, Kollman PA, Case DA. Development and testing of a general

amber force field. J Comput Chem [Internet]. 2004 Jul 15;25(9):1157–74. Available from: https://doi.org/10.1002/jcc.20035

38. Jorgensen WL, Chandrasekhar J, Madura JD, Impey RW, Klein ML. Comparison of simple potential functions for simulating liquid water. J Chem Phys [Internet]. 1983 Jul 15;79(2):926–35. Available from: https://doi.org/10.1063/1.445869
39. Mai S, Gattuso H, Monari A, González L. Novel Molecular-Dynamics-Based Protocols for Phase Space Sampling in Complex Systems [Internet]. Vol. 6, Frontiers in Chemistry . 2018. p. 495. Available from: https://www.frontiersin.org/article/10.3389/fchem.2018.00495
40. Segalina A, Cerezo J, Prampolini G, Santoro F, Pastore M. Accounting for Vibronic Features through a Mixed Quantum-Classical Scheme: Structure, Dynamics, and Absorption Spectra of a Perylene Diimide Dye in Solution. J Chem Theory Comput [Internet]. 2020 Nov 10;16(11):7061–77. Available from: https://doi.org/10.1021/acs.jctc.0c00919
41. Cerezo J, Aranda D, Avila Ferrer FJ, Prampolini G, Santoro F. Adiabatic-Molecular Dynamics Generalized Vertical Hessian Approach: A Mixed Quantum Classical Method To Compute Electronic Spectra of Flexible Molecules in the Condensed Phase. J Chem Theory Comput [Internet]. 2020 Feb 11;16(2):1215–31. Available from: https://doi.org/10.1021/acs.jctc.9b01009
42. Avagliano D, Tkaczyk S, Sánchez-Murcia PA, González L. Enhanced Rigidity Changes Ultraviolet Absorption: Effect of a Merocyanine Binder on G-Quadruplex Photophysics. J Phys Chem Lett [Internet]. 2020 Dec 3;11(23):10212–8. Available from: https://doi.org/10.1021/acs.jpclett.0c03070
43. Suchan J, Hollas D, Curchod BFE, Slavíček P. On the importance of initial conditions for excited-state dynamics. Faraday Discuss [Internet]. 2018;212(0):307–30. Available from: http://dx.doi.org/10.1039/C8FD00088C